Protein Science (1996), 5:836-851. Cambridge University Press. Printed in the USA.

Structural investigation of the alpha-1-antichymotrypsin: prostate-specific antigen complex by comparative model building

BRUNO O. VILLOUTREIX,[1] HANS LILJA,[2] KIM PETTERSSON,[3] TIMO LÖVGREN,[3] AND OLLE TELEMAN[1]

[1] Technical Research Centre of Finland, VTT Biotechnology and Food Research, POB 1500, FIN-02044 VTT (Espoo), Finland
[2] Department of Clinical Chemistry, Lund University, University Hospital, Malmö, Sweden
[3] University of Turku, Department of Biotechnology, Fin-20520 Turku, Finland

(RECEIVED December 5, 1995; ACCEPTED February 22, 1996)

Abstract

Prostate-specific antigen (PSA), produced by prostate cells, provides an excellent serum marker for prostate cancer. It belongs to the human kallikrein family of enzymes, a second prostate-derived member of which is human glandular kallikrein-1 (hK2). Active PSA and hK2 are both 237-residue kallikrein-like proteases, based on sequence homology. An hK2 model structure based on the serine protease fold is presented and compared to PSA and six other serine proteases in order to analyze in depth the role of the surface-accessible loops surrounding the active site. The results show that PSA and hK2 share extensive structural similarity and that most amino acid replacements are centered on the loops surrounding the active site. Furthermore, the electrostatic potential surfaces are very similar for PSA and hK2.

PSA interacts with at least two serine protease inhibitors (serpins): alpha-1-antichymotrypsin (ACT) and protein C inhibitor (PCI). Three-dimensional model structures of the uncleaved ACT molecule were developed based upon the recent X-ray structure of uncleaved antithrombin. The serpin was docked both to PSA and hK2. Amino acid replacements and electrostatic complementarities indicate that the overall orientation of the proteins in these complexes is reasonable. In order to investigate PSA's heparin interaction sites, electrostatic computations were carried out on PSA, hK2, protein C, ACT, and PCI. Two heparin binding sites are suggested on the PSA surface and could explain the enhanced complex formation between PSA and PCI, while inhibiting the formation of the ACT-PSA complex. PSA, hK2, and their preliminary complexes with ACT should facilitate the understanding and prediction of structural and functional properties for these important proteins also with respect to prostate diseases.

Keywords: antichymotrypsin; coagulation; electrostatic potential; human glandular kallikrein-1; prostate cancer; prostate-specific antigen; protein C; protein C inhibitor; protein modeling; serine protease; serpin

Reprint requests to: Bruno O. Villoutreix, Technical Research Centre of Finland, VTT Biotechnology and Food Research, POB 1500, FIN-02044 VTT (Espoo), Finland; e-mail: villoutr@bel.vtt.fi.

Abbreviations: P1, P2, P3... and P'1, P'2... designate inhibitor residues amino- and carboxy-terminal to the scissile peptide bond, respectively, and S1, S2... and S'1, S'2... the corresponding subsites of the protease (Schechter & Berger, 1967). The chymotrypsinogen nomenclature is used (Bode et al., 1989). The PSA/hK2 numbering is indicated between brackets whenever appropriate. The protein C numbering is provided between parentheses when appropriate. CHA, bovine chymotrypsin; TLD, bovine trypsin; TON, rat tonin; PKA, porcine kallikrein; THR, human thrombin; PC, human protein C; APC, activated PC; ATIII, human antithrombin; AT, human antitrypsin; PCI, human protein C inhibitor; ACT, human α_1-antichymotrypsin; BPTI, bovine pancreatic trypsin inhibitor. The numbering of ACT in this work follows the conventions established for α_1-antitrypsin (Huber & Carrell, 1989).

Prostate-specific antigen (PSA or hK3) and human prostatic glandular kallikrein (hK2 or hGK-1) are serine proteases, and two of a total of three members in the glandular kallikrein gene family in man (Riegman et al., 1992). The expression of PSA and hK2 is androgen dependent but not uniquely restricted to prostate tissue, because both proteins are also expressed at low levels in several non-prostatic tissues (Henttu et al., 1990; Young et al., 1992; Clements & Mukthar, 1994; Monne et al., 1994; Yu & Diamandis, 1995). The primary structure of PSA shares 79% identity with that of hK2 and the polypeptide chain of each protein contains 237 amino acid residues and a single Asn-linked carbohydrate chain (Lundwall & Lilja, 1987; Schaller et al., 1987; Schedlich et al., 1987; Bélanger et al., 1995).

The single-chain form of PSA manifests chymotrypsin-like substrate specificity in this action, because it has been shown to

hydrolyze peptide bonds C-terminal of certain tyrosine and leucine residues in semenogelin I (Akiyama et al., 1987; Lilja et al., 1989; Christensson et al., 1990). The primary structure of hK2 suggests it to be a trypsin-like protease (Schedlich et al., 1987), but its physiological function remains to be understood.

The active single-chain form, constituting 70% of PSA in seminal fluid, slowly forms stable, covalent complexes with several extracellular proteinase inhibitors in vitro, such as α_2-macroglobulin (AMG), pregnancy-zone protein (PZ-protein, an AMG-analogue), and the serpin-superfamily members α_1-antichymotrypsin (ACT) and protein C inhibitor (PCI) (Christensson et al., 1990; España et al., 1991; Christensson & Lilja, 1994). Because the molar levels of PSA in the seminal fluid is 10 times that of PCI, typically only 5% of PSA is complexed to PCI (España et al., 1993; Christensson & Lilja, 1994).

The mainly liver-derived ACT and AMG normally occur at 10^4–10^5-fold molar excess to PSA in serum. However, most, if not all immunoassays fail to recognize the PSA-AMG complex. By contrast, several independent antigenic epitopes remain exposed on the PSA moiety of the PSA-ACT complex that can interact with poly- or monoclonal anti-PSA IgGs (Christensson et al., 1990; Lilja et al., 1991).

Prostate disease, in particular prostate cancer (CAP), results in breakdown of the barriers provided by the basal membrane of the glandular ducts that normally prevent escape of PSA into the blood. This results in PSA elevations in serum. However, benign conditions, such as bacterial prostatitis, urinary retention, and benign prostatic hyperplasia (BPH) may also result in the release of elevated PSA levels in serum (Oesterling, 1991).

In 1991, it was first shown that PSA complexed to ACT was the predominant form of the immunoaccessible PSA in serum, and that the proportion of PSA-ACT complex to that of the total PSA in serum was higher in CAP patients than in those with BPH alone (Lilja et al., 1991; Stenman et al., 1991; Christensson et al., 1993; Leinonen et al., 1993). The proportion of free, noncomplexed form of PSA to that of total PSA was significantly higher in BPH than in CAP and was strongly suggested to provide an efficient means to more reliably distinguish CAP from BPH (Christensson et al., 1993). The production of both recombinant hK2 and PSA have been used to study in detail the antigenic epitopes defined by monoclonal anti-PSA IgGs and have shown that the antigenic epitopes on the free PSA in serum are unique to PSA alone, and do not cross-react with the extensively similar hK2 (Lövgren et al., 1995; Pettersson et al., 1995). Thus, in order to investigate further the results of the PSA-ACT epitope mapping data, we have undertaken molecular modeling studies of the different PSA–serpin complexes.

In the absence of crystallographic or NMR structural information, homology modeling provides a useful approach to addressing structure–function questions (Furie et al., 1981; Blundell et al., 1987; Greer, 1990; Cohen et al., 1991; Hedstrom et al., 1992; Fernández et al., 1994; Sunnerhagen et al., 1995). Recently, several model structures have been developed for PSA and hK2 molecules (Vihinen, 1994; Villoutreix et al., 1994a; Bridon & Dowell, 1995) and the presented data shown to be complementary. The current study compares in depth the model structures of PSA and hK2, the loop structures surrounding the active site, and describes a three-dimensional model of uncleaved ACT. Possible interactions between the uncleaved ACT and PSA were investigated on the basis of surface complementarities and potential PSA heparin interaction site(s) are suggested. The discussion includes comparison of the possible residues in contact between ACT and PSA, as well as hK2 and ACT (there is yet no evidence of an hK2-ACT complex).

Results and discussion

Sequence and structural alignment: Serine proteases

The serine proteases are widely distributed in nature, where they perform a variety of functions. Many three-dimensional structures and sequences of this family are known, thus making comparative model building easier and improving the accuracy of predicted structures (Greer, 1990).

Structural and sequence alignments (models and X-ray structures) of eight serine proteases were carried out (Fig. 1). The sequence identity is high in the areas surrounding the catalytic triad and within the structurally conserved regions. Interesting differences occur within the variable regions and offer means to make the enzyme specific for a particular substrate or inhibitor.

Overall structure of the serine proteases

The serine proteases consist of two domains each formed by a six-stranded antiparallel β barrel with the active site located in a cleft between these two domains (Figs. 1, 2). We will refer to these domains as domain A, which includes the catalytic residues Asp 102 and His 57, and domain B, which possesses the last residue of the catalytic triad, Ser 195. Domain B also contains the residues forming the specificity pocket (loop 7 and 8) and main-chain substrate binding residues (residues 214–216) (Figs. 1, 2). In addition, these proteins usually contain four to six disulfide bridges, and five of these are conserved in PSA and hK2. The differences between these structures are concentrated in surface loops, mainly located around the active site, and are in part responsible for the different reactivities and specificities.

Comparison and evaluation of the PSA and hK2 model structures

The sequence of porcine kallikrein is identical to that of PSA to about 55% and to 64% with that of hK2. The sequence identity between PSA and hK2 is about 79%. This suggests that hK2 and PSA are closely related in terms of three-dimensional structure and also very similar to the kallikrein X-ray structure except for some surface loops. A three-dimensional model for the structure of hK2 was built by homology modeling. In the hK2 model, all residues expected to be of importance for stabilizing the structure are strictly conserved (e.g., disulfide bridges, hydrophobic, and charge–charge interactions). Most of the side-chain replacements in hK2 are conservative compared to those in PSA. Nonconservative replacements of interest are mentioned below.

Residue Leu 32 [17] in the PSA sequence is replaced by an Ala in hK2. The shorter side chain accommodates the nearby replacement of Ala 34 [19] in PSA by a Tyr in hK2. This Tyr side chain interacts favorably with the nearby Trp 66 [50], which is a Leu in PSA. In the active site region (loop 1), we note the replacement of Arg 39 [23] of PSA by a solvent-accessible Trp in hK2. This residue may have some importance for the interaction with substrates or inhibitors (see below). Val 64 [48] in PSA is replaced in hK2 by a solvent-accessible Gln. This residue is likely

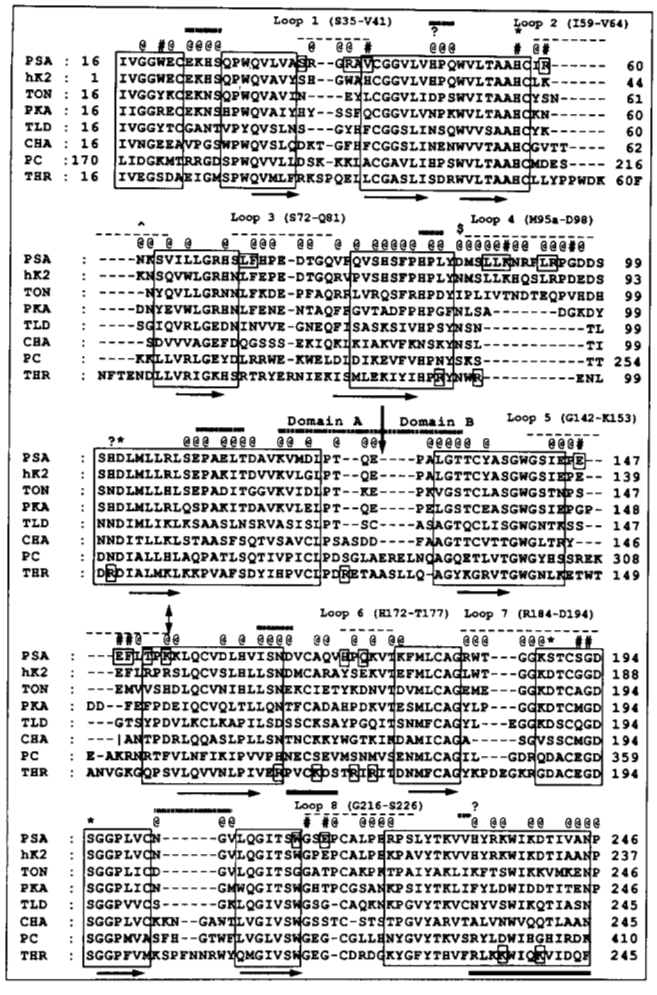

Fig. 1. Sequence and structural alignment of eight serine proteases. The sequences of human prostate specific antigen (PSA), human glandular kallikrein-1 (hK2), rat tonin (TON), porcine kallikrein (PKA), bovine trypsin (TLD), bovine chymotrypsin (CHA), human protein C (serine protease domain, PC), and human thrombin (THR) were aligned according to the structurally conserved regions, which are delineated by black boxes. Asterisk indicates the catalytic triad residues (His 57 [41], Asp 102 [96], and Ser 195 [189]), as well as the residue at the bottom of the specificity pocket, Ser or Asp 189 [183]. The @ symbol above the sequences depicts solvent-accessible side chains of PSA in its complexed form with ACT (see the Materials and methods) and the # symbol depicts the residues becoming inaccessible upon formation of this complex. The ? symbol represents the residues of PSA suggested to form (at least in part) a zinc ion binding site (His 91 [74], 101 [95], 233 [224]). The ^ and $ symbols represent the glycosylation sites in PSA (residue Asn 61 [45]) and hK2 (residue Asn 95 [78]), respectively. The double-headed arrow represents a cleavage site in PSA (between Lys 153 [145] and 154 [146]) and the short vertical arrow (↓) shows approximately the end of domain A (first β-barrel, His 57 and Asp 102, C-terminal helix) on the back side of the molecule and the beginning of the domain B (N-terminal region, second β-barrel, Ser 195, and the specificity pocket). PSA is also cleaved at Arg 95g [85] and Lys 188 [182] (not shown). The loops surrounding the active site are shown by a thin dashed line above the sequence, some of the residues of loop 8, among others, play an important role for substrate specificity, Gly 216 [206] and Ser 226 [217] in PSA. Just preceding this loop are the residues involved in the main-chain binding of the substrates, Ser 214 [204] to Gly 216 [206]. The | symbol in the CHA sequence before residue Ala 149 indicates the cleavage site in the autolysis loop (the uncleaved sequence is $Y_{146}TNA_{149}$). The residues of the "kallikrein loop" (Loop 4) in tonin are listed, although no crystallographic information is available for this part of the molecule. A cleavage occurs at the corresponding position in PKA and it is not known how many residues are missing. The thick dashed line above the sequences indicates some solvent-accessible residues on the opposite side of the binding site. The small black boxes in the PSA sequence indicate the loops' residues of PSA interacting with ACT (the catalytic triad and specificity pocket residues are not included because they are already marked by asterisks). Similar boxes in thrombin indicate some of the heparin-binding residues. Beneath the sequences, black arrows represent the β-strands in the PSA model and the solid black lines the α-helices. Chymotrypsinogen numbering is maintained throughout this sequence alignment and the PSA numbering can be seen in the hK2 sequence. The protein C numbering was kept to help in comparing the data from the literature and was taken from the PDB file.

to interact with Arg 82 [65] in hK2, which replaces a Val in the PSA sequence. At the surface of hK2, Asn 72 [55] replaces a Ser in PSA and, nearby, the hK2 Glu 75 [58] replaces a His in PSA, thus making possible hydrogen bonding. Gly 96 [90] in PSA is replaced by an Asp in hK2. This residue is solvent accessible and is close to three other negatively charged residues, Glu 97 [91] (Asp in PSA), Asp 98 [92] (conserved in PSA), and Glu 174 [166] (Gln in PSA). Asp 98 [92] in PSA and hK2 are likely to interact with the side chain of the conserved Lys 175 [167]. This region of hK2 is more negatively charged than in PSA. The solvent-accessible Glu 113 [107] in PSA is replaced by a Lys in hK2. This replacement is far from the binding site and should not be involved in substrate-inhibitor recognition. Replacement of the solvent-accessible Asp 122 [116] of PSA by a Gly residue in hK2 was straightforward. This residue is located on the opposite side of the molecule and lacks strong interactions with its surrounding. Replacement of Thr 151 [143] of PSA by an Arg residue in hK2 may play a role in substrate–inhibitor specificity because it is close to the active site (loop 5). This Arg 151 [143] has its side chain relatively close to Arg 153 [145] in hK2 (Lys 153 in PSA), this area of the active site cleft is thus more positive in hK2 than in PSA. Replacement of the solvent-accessible Lys 154 [146] of PSA by a Ser in hK2 did not create any problem. This Ser in hK2 is likely to interact with the conserved Glu 21 [6] or with Asn 72 [55] of hK2. Replacement of Asp 159 [151] of PSA by a Ser in hK2 was straightforward. This residue is far from the active site and probably forms a salt bridge in PSA with the conserved Lys 188 [182]. Nevertheless, hydrogen bonding is most likely in hK2 between Ser 159 [151] and Lys 188 [182]. Replacement of Gln 170 [162] of PSA by an Arg in hK2 was well accommodated. This solvent-accessible residue is far from the active site and can interact with the conserved solvent-accessible Glu 223 [214] and Asp 166 [158]. The solvent-exposed Lys 178 [170] of PSA is replaced by a Glu in hK2. This residue is far from the active site region. Arg 184 [177] of PSA is replaced by a Leu in hK2. This hydrophobic residue is partially accessible to the surface, but still has hydrophobic contacts with the carbon side chain of the conserved Lys 188 [182] and Thr 186 [179]. Replacement of Ser 189 [183] of PSA by an Asp in hK2, at the bottom of the specificity pocket, was also straightforward. This residue should play a major role for substrate–inhibitor specificity.

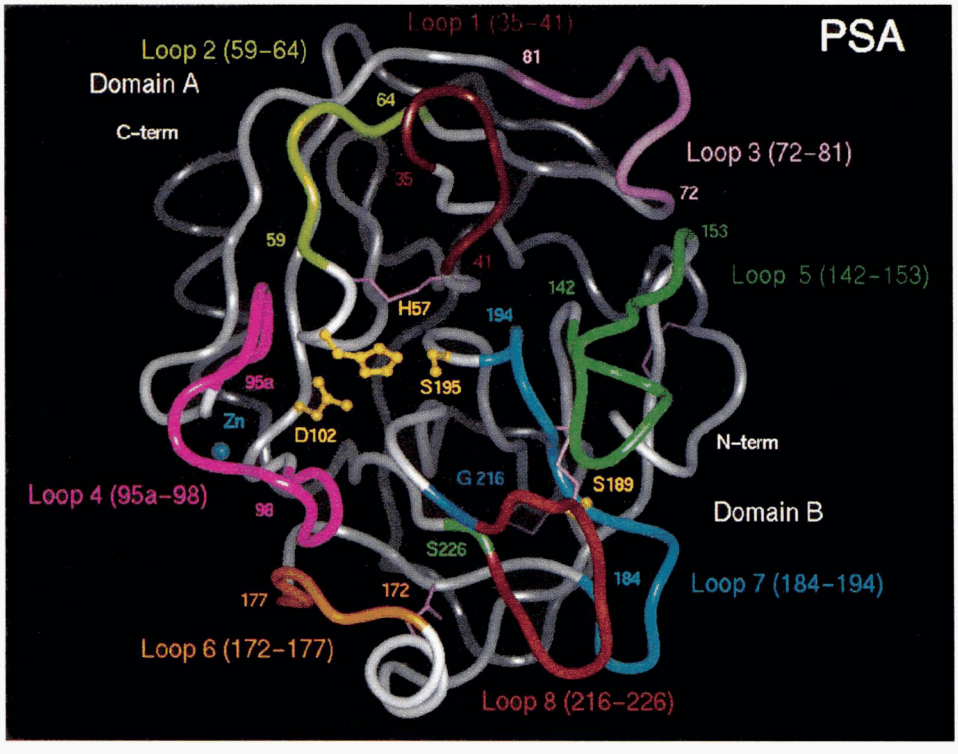

Fig. 2. The prostate-specific antigen model structure. The model is shown in ribbon drawing with a view down the active site. Residues belonging to the active site triad are shown in ball and stick representation (yellow). This triad involves the nucleophilic serine 195 [189], the nearby His 57 [41], and the Asp 102 [96]. Also shown is the residue at the bottom of the specificity pocket, Ser 189 [183] in the case of PSA. This residue is an aspartate in hK2. The loops defined in Figure 1 are shown in different colors. They involve residues 35 [20] {188}–41 [25] {195 in PC} for loop 1; 59 [43] {213}–64 [48] {220} for loop 2; 72 [55] {227}–81 [64] {236} for loop 3; 95a [79] {251}–98 [92] {253} for loop 4; 142 [134] {301}–153 [145] {316} for loop 5; 172 [164] {335}–177 [169] {340} for loop 6; 184 [177] {348}–194 [188] {359} for loop 7; and 216 [206] {281}–226 [217] {391} for loop 8. Important residues at the entrance of the specificity pocket are colored dark blue (Gly 216 [206]) and green (Ser 226 [217]). In hK2, these residues are Gly 216 and Ala 226, respectively. The disulfide bridges are drawn as light pink sticks, but are not labeled. These involve Cys 42 [26] with Cys 58 [42] at the level of loop 1 and loop 2; Cys 22 [7] with Cys 157 [149], connecting the N-terminal region with the β-strand following loop 5, to the right of the figure; Cys 191 [185] with Cys 220 [210], connecting loop 7 and loop 8, seen just next to Ser 189; at the back of the molecule, Cys 136 [128] with Cys 201 [195], this is seen behind loop 8 and appears to go from Ser 189 to Gly 216; finally, just behind loop 6, Cys 168 [160] with Cys 182 [174]. The postulated zinc ion-binding site of PSA involving at least His 91 [74] (in the sequence PHPLY), 101 [95] (in SSHD) and 233 [224] (in VVHY) is marked by the presence of a blue sphere at the base of loop 4, which represents a manually docked zinc ion. These three His residues are conserved in hK2.

Thus, as in other protein families, most of the nonconservative side-chains replacements in hK2, when compared to PSA, are fully accessible to the surface.

Spatially correlated mutations have been noted as very important for the validity of a homology model (Struthers et al., 1991) and are present in the hK2 and PSA models as compared with the structure of porcine kallikrein, but are also present between PSA and hK2. Moreover, several conserved charge–charge interactions between the kallikrein X-ray structure and the PSA model (Villoutreix et al., 1994a) are also present in hK2. These conserved interactions are Asp 116 [110]–Lys 119 [113], Lys 175 [167]–Asp 98 [92], Lys 24 [9]–Glu 77 [60], Lys 230 [221]–Glu 128 [121], Arg 70 [53]–Glu 77 [60]. In addition, the conservation of the five disulfide bridges between kallikrein, PSA, and hK2 (Cys 42 [26]–Cys 58 [42] in domain A and Cys 22 [7]–Cys 157 [149], Cys 136 [128]–Cys 201 [195], Cys 168 [160]–Cys 182 [174], Cys 191 [185]–Cys 220 [210] in domain B) are strong indications that the overall three-dimensional structure of the proteins is conserved. Together with the fact that no major steric clashes appeared during the construction of PSA and hK2 model structures, the above results provide strong evidence for the validity of these models. However, ambiguities remain in the area of loop 4 (Villoutreix et al., 1994a).

The overall distribution of charges is relatively similar in PSA and hK2, with positively charged residues mainly located in domain A, at the tips of some surface loops. Negatively charged residues are mainly located in domain B and the base of loop 4, more inside the active site cleft. The differences are slightly larger when comparing electrostatic isopotential contours (see below). None of the two molecules contains significant solvent-accessible hydrophobic clusters.

Interestingly, several of the side-chain replacements between PSA and hK2 are located in the vicinity of the active site. These replacements can be seen in all eight loops as defined in Figure 1. Some of these substitutions may be of importance for substrate specificity or recognition. By comparison, very few substitutions occur on the back side of the molecule (opposite to the binding area).

Analysis of the loops surrounding the active site of eight selected serine proteases

Figure 1 gives the alignment of eight serine proteases. The structural differences between these proteins are concentrated to surface loops, mainly around the active site. We here analyze the overall similarities and differences between the loops of these enzymes. This structural analysis of the loops surrounding the active site provides the basis for the initial docking experiments of a serpin into the binding cleft of a serine protease.

Loop 1 (residues 35 [20]–41 [25], see also the legend of Figure 2 for the PC numbering). The overall C_α trace of this loop is the same in all the X-ray structures, whereas a more detailed analysis shows local differences. Interestingly, tonin is the only protein showing a bend in this loop such that the side chain of Glu 39 [23] and Tyr 40 [24] occupy totally different positions compared to the other seven proteases. Here, hK2 possesses a large hydrophobic side chain, Trp 39 [23], which is likely to play a role in the binding of substrates or macromolecular inhibitors. PSA, protein C, and thrombin display several charged residues in this area that could play a role in substrate/inhibitor binding (Fig. 1). In all eight proteins, the part of the loop closer to the binding site cleft (residues 38 [22]–41 [25]) is held by a disulfide bond involving Cys 42 [26] and Cys 58 [42] of loop 2, which makes the base of this loop probably rigid.

Loop 2 (residues 59 [43]–64 [48]) has an overall similar C_α structure in seven proteins, whereas thrombin shows an insertion of about 10 residues. In thrombin, this loop projects out of the surface of the molecule and seems to be relatively rigid, as pointed out by Bode et al. (1992). This loop is glycosylated at Asn 60g (DKNFT), but this has no apparent effect on substrate binding. This loop has also been suggested to interact with the core structure of antithrombin (Bode et al., 1992). When superimposing the X-ray structure of thrombin and the PSA model, thrombin residues Pro 60b and 60c clash sterically with Ser 95b [80], Leu 95c [81] of loop 4 of PSA. Loop 4 of PSA interacts with the core of antichymotrypsin in our modeled complex and thus could play a role similar to that of loop 2 of thrombin. Loop 2 of PSA is glycosylated at Asn 61 [45], which is fully solvent accessible in the model structure (Villoutreix et al., 1994a). This glycosylation site is not conserved in hK2, which instead possesses one in loop 4, residue Asn 95 [78]. The physiological importance of this carbohydrate in PSA is unknown.

Loop 3 (residues 72 [55]–81 [64]) shows a similar overall C_α structure similar in all eight proteases, however, a detailed analysis reveals differences. This loop binds a calcium ion in the case of bovine trypsin or factor IX as well as in several other serine proteases (Meyer et al., 1988). In trypsin, it has been shown that the integrity of this loop confers thermal stability to the whole molecule (Bode, 1979). Fisher et al. (1994) suggested that this loop is also involved in calcium binding in protein C, and Greengard et al. (1994) showed that a mutation of a nearby Arg 178 (corresponding to residue 24 [9] in the chymotrypsinogen/PSA numbering) leads to a Type I deficiency, probably due to the destabilization of the molecule. In thrombin, this loop is stabilized by a cluster of salt bridges, mainly buried in the molecule, and does not interact with calcium (Bode et al., 1989). The environment in thrombin is mainly positively charged (anion binding exosite I) (Bode et al., 1992). In PSA, the loop is also likely to be stabilized by salt bridges (Villoutreix et al., 1994a). The residues involved are Glu 77 [60] with Arg 70 [53] and Lys 24 [9]. These residues are conserved in hK2 and PKA and are likely to form a similar pattern of interactions.

Loop 4 (residues 95a [79]–98 [92]) shows differences within these eight molecules. PSA, hK2, and tonin have a large insertion. It is also likely that kallikrein has a large insertion in loop 4 (Fujinaga & James, 1987). Because no appropriate template coordinates were available to build loop 4, the loop, commonly called "the kallikrein loop," has been built de novo (Villoutreix et al., 1994a). The uncertainty of the PSA and hK2 structures is high in this area. It is important to note that this loop seems to interact with a serpin molecule in the case of PSA and hK2, and that the starting conformation used in this work (see the Materials and methods) had to be opened up manually in order to allow the docking of the serpin molecule. We have suggested previously that this loop is flexible (Villoutreix et al., 1994a). In PSA, this loop can be cleaved after residue Arg 95g [85] (Watt et al., 1986). The part of the tonin loop defined by X-ray studies shows significant differences from the visible portion of the same loop in kallikrein. These differences are probably due to the difference in length and the fact that, in tonin, this loop binds a zinc ion (Fujinaga & James, 1987). In hK2, residue Asn 95 [78] is glycosylated. This residue is fully solvent accessible and can make a hydrogen bond with the nearby Lys 175 [167]. This loop in thrombin and its environment (anion binding exosite II) have been shown to be involved in heparin binding (Sheehan & Sadler, 1994).

Loop 5 (residues 142 [134]–153 [145]) of the PSA and hK2 models are likely to be similar to the one observed in tonin rather than the one of kallikrein, mainly due to the fact that PSA, hK2, and tonin have a loop of same length and of relatively high sequence similarity. In human protein C, this loop is four residues longer than in PSA. It can be hypothesized that this loop in protein C is flexible, as in the case of thrombin. Preliminary model building of APC-PCI suggests that significant sterical hindrance occurs upon docking of the serpin molecule. In consequence, this loop in PC probably opens up on interaction with a macromolecular inhibitor, although the serpin can also be tilted toward the protease domain A. In thrombin, this loop is much longer than in PSA or hK2. A cleavage site is present in PSA between residue Lys 153 [145] and Lys 154 [146], and upon cleavage the molecule becomes enzymatically inactive (Christensson et al., 1990).

Loop 6 (residues 172 [164]–177 [169]) has a conserved length in all eight proteins. However, the structure shows interesting differences, mainly for residues 172–175. One of the reasons for these structural changes is the difference in length and/or orientation of the α-helix directly preceding this loop (Fig. 1). For example, this α-helix segment in kallikrein is replaced by two short 3_{10} helices in tonin (Fujinaga & James, 1987). This region in PSA is likely to be similar to that of kallikrein, mainly due to the conservation of Pro 173 [165]. This residue is a serine [165] in hK2, but modeling experiments suggest that this part of hK2 is more likely to have a structure similar to that of porcine kallikrein rather than tonin. This region, referred to as "loop 4" in Brillard-Bourdet et al. (1995), is suspected to contribute to the P4–P7 substrate specificity in rat tissue kallikrein.

Loop 7 (residues 184 [177]–194 [188]) and **Loop 8** (residues 216 [206]–226 [217]) form the S1 binding pocket. These two loops are held together by a disulfide bridge involving Cys 191 [185] and Cys 220 [210], thus making this region of the protein

relatively rigid. Differences in length and in the amino acid composition of this area play a major role in substrate specificity. The residue at the bottom of the specificity pocket is an Asp (residue 189 [183]) in all but PSA and chymotrypsin, which contain a serine. This has been shown to contribute to substrate specificity (Bode & Huber, 1992). In fact, an aspartate residue at position 189 confers trypsin-like specificity, thus cleaves preferentially after an arginine or lysine, whereas a serine at position 189, confers chymotrypsin-like activity (Bode & Huber, 1992). The other key amino acids are residues 190 [184], 192 [186], 216 [206], and 226 [217], because they are located at the entrance of the specificity pocket and can alter the access of the P1 residue side chain. Another important residue in PSA, hK2, tonin, and kallikrein is proline 219 [209]. This proline residue assumes a *cis* configuration in kallikrein and tonin and apparently contributes to the enlargement of the binding pocket (Chen & Bode, 1983). This residue is conserved in PSA and hK2, and it can be assumed that its peptide geometry is likely to be *cis*. In PSA, this loop can be cleaved after residue Lys 188 [182] (Watt et al., 1986, in their paper this Lys is referred to as residue 185). The PSA Ser 192 [186] is Gly in hK2, which tends to enlarge the hK2's pocket entrance. This residue may be of importance because Glu 192 seems to selectively restrict thrombin's ability to accept Met as the P1 residue (Le Bonniec et al., 1995).

Loop 8 shows some structural variation. The most significant change observed is in tonin, where the C_α trace of loop 8, from residue Gly 215 [205] to Cys 220 [210], adopts a very different conformation, closing off the specificity pocket (Fujinaga & James, 1987).

An extensive discussion of the interactions of enzymes-inhibitors involving loops 7 and 8 can be found in Bode and Huber (1992) and Perona and Craik (1995) and thus will not be presented here. In summary, it would appear that, in PSA, the "wall" surrounding the active site is more pronounced at loop 4 and to some extent at loop 6, compared to thrombin, whereas the latter has much longer loops 1, 2, and 5. These observations for thrombin tend to hold also for protein C. Chymotrypsin has longer loops 1 and 2, a different conformation for loop 3, a much shorter loop 4, a more open loop 6, and shorter loops 7 and 8 than PSA.

Overall structure of the serpin molecules

The serine proteinase inhibitors (serpins) form a family of homologous and large, generally glycosylated, proteins comprising about 400 residues. As in the case of the smaller canonical inhibitors (Kunitz, Kazal, etc.), serpins seem to interact with the proteinases through an exposed binding loop, but undergo cleavage rather than only binding. The serpins are made up of two layers of β-pleated sheets partly covered by α-helices. It is expected that the so-called reactive loop, which is responsible for protease recognition and specificity, protrudes from their surfaces. In this protein family, part of the reactive loop is inserted into the β-sheet A (strand 4A) after cleavage. The residues P1 and P'1 are then separated by about 70 Å. The serpin superfamily exhibits remarkable three-dimensional structural conservation despite the fact that the sequence identity can be relatively low (Huber & Carrell, 1989). This structural conservation allows reliable sequence alignment and therefore accurate homology modeling experiments.

The crystal structures of ovalbumin (Stein et al., 1990, 1991) and its nicked form plakalbumin (Wright et al., 1990) have been determined. In ovalbumin, the reactive loop is mainly α-helical, amounting to a useful initial guide-line for modeling purposes (Stein et al., 1990). It is expected that this helical structure unfolds rapidly in order to fit the active site of the protease (Stein et al., 1990). An uncleaved form for antithrombin has been studied recently by X-ray crystallography (Carrell et al., 1994; Schreuder et al., 1994) and seems more appropriate for the modeling of an uncleaved serpin in its active conformation. However, in this X-ray structure, the P1 residue points toward the serpin core. In order to be cleaved, the P1 residue must be accessible, and thus the reactive loop probably adopts an intermediate canonical conformation as observed in small serine protease inhibitors. By contrast with ovalbumin, the uncleaved ATIII has two residues pre-inserted in the sheet A.

In order to investigate the possible interactions between PSA, hK2 on one hand, and ACT on the other hand, we built a model of the uncleaved form of this serpin and docked it into the active site of our newly built PSA and hK2 models. Figure 3 shows the structural and sequence alignment of four members of the serpin family. Residues accessible to the surface, secondary structure elements, heparin-binding residues in antithrombin, as well as residues expected to be involved in the PSA-ACT interaction or within 12 Å of a protease are mentioned.

Evaluation of the uncleaved antichymotrypsin model

The uncleaved ACT model was built using the following steps: (1) removing the strand A4 from the sheet A; (2) building the reactive loop using the X-ray structure of uncleaved antithrombin as template; (3) minimizing the structure and changing the orientation of four residues around the P1 residue in order to correspond to the canonical structure observed in small protease inhibitors; (4) short runs of minimization with restraints and molecular dynamics were performed in order to partially reproduce hydrogen bonding between strands 3A and 5A.

Katz and Christianson (1993) developed a model of uncleaved ACT based on the structure of ovalbumin and optimized it by molecular mechanics and dynamics. The overall structure of our ACT model structure should be similar to their model, although the reactive loop and β-sheet A will obviously be somewhat different due to different methodology and template. Wei et al. (1994) recently determined an X-ray structure of a variant of human antichymotrypsin. This structure contains an intact reactive loop in a distorted helical conformation and strand A4 is not pre-inserted into sheet A. In this structure, the reactive loop does not seem optimal for interaction with the serine protease active site, although local rearrangement may occur upon binding. Reviews of the different hypotheses regarding the structure of the reactive loop and the pre-insertion region are found in Wei et al. (1994) and Carrell et al. (1994). In this paper, we have assumed that the reactive loop will be similar to the one observed in the X-ray structure of uncleaved antithrombin.

The minimized potential energy obtained for ACT is similar to those obtained for large properly folded proteins. Also, the distributions of charged and hydrophobic residues, which are generally more sensitive indicators of model validity, were found to agree with those obtained from experimentally determined protein structures. Furthermore, because the structural rearrangement between an uncleaved and cleaved serpin is mainly

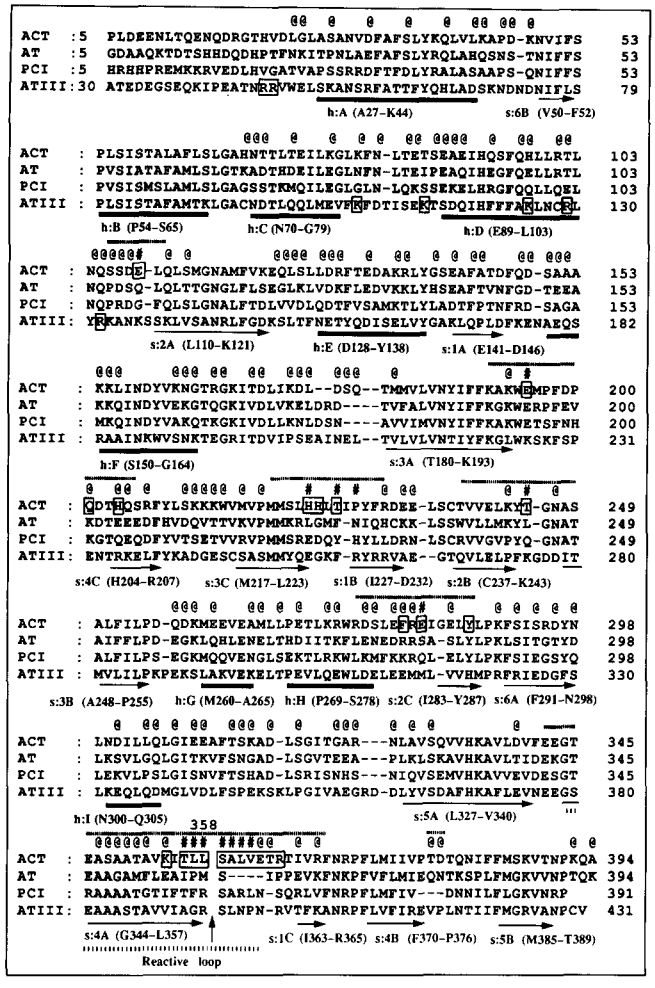

Fig. 3. Sequence and structural alignment of four serpin molecules. The sequences of human α_1-antichymotrypsin (ACT), human α_1-antitrypsin (AT), human antithrombin (ATIII), and human protein C inhibitor (PCI) were aligned manually according to the structurally conserved regions as described by Huber and Carrell (1989). The @ symbol above the ACT sequence denotes solvent-accessible side chains of the uncleaved minimized ACT model in its complexed form with PSA (see the Materials and methods), and the # symbol shows the residues becoming inaccessible upon complex formation. The small black boxes in the ACT sequence indicate the residues of ACT interacting directly with PSA. In the ATIII sequence, similar boxes indicate some of the heparin-binding residues. Beneath the sequences, the black arrows represent the β-strands in the cleaved ACT X-ray structure and the solid black lines, the α-helices. Residues involved in the secondary structure elements of ACT are mentioned in parentheses. The dotted line represents the reactive loop in ACT, i.e., from Gly 344 (P17) to Glu 359d (P'5). The short vertical arrow (↑) represents the major cleavage site in the serpin superfamily of proteins. Above the sequence, the thick dashed line indicates residues at 12 Å from PSA in the PSA-ACT model complex. AT inhibitor numbering is maintained throughout this sequence alignment (Huber & Carrell, 1989) and the numbering of ATIII was taken from the PDB file.

localized to the A sheet and reactive loop, our overall model structure for ACT is certainly reasonable.

At the beginning of the reactive loop, in the sheet A, residues Glu 377 and 378 form a β-turn in the uncleaved structure of ATIII. They interact with Arg 322 and Lys 228, respectively. Three residues further, Glu 381 interacts with Lys 222. The ATIII Ser 380 side chain is still in sheet A, whereas the loop leaves it at an almost perpendicular angle. In ACT, the counterpart of Ser 380 is Thr 345, which can have the same orientation as ATIII Ser 380 without creating steric clashes. The Glu 377–Arg 322 salt bridge of ATIII has an exact counterpart between Glu 342 and Lys 290 in ACT. The interaction between Glu 378 and Lys 228 of ATIII is replaced in ACT by interaction between the conserved Glu, at position 343 with Lys 193, which corresponds to Leu 224 in ATIII. The interaction Glu 381–Lys 222 of ATIII is conserved in ACT and involves Glu 346–Lys 191. After this position, the reactive loop has several residues with short side chains and reaches the P5 residue, where structural differences between the X-ray structure of ATIII and the ACT model are relatively important. Thus, it seems that the pre-insertion area can be structurally conserved in ACT as compared with ATIII.

In order to dock ACT in the active site of PSA and hK2 and avoid clashes with loop 1, it was necessary to slightly open the strand 1 of sheet C. Arg 361, Thr 362, and Ile 363 of ACT, which are normally part of sheet C, were then slightly too far for main-chain hydrogen bonding with strand 2C. This can be modified either by slightly moving loop 1 or by tilting ACT toward loops 4 and 6 of the protease.

Model building of the ACT-PSA complex and the reactive loop of ACT

From the complexes of serine proteases with small protease inhibitors (Bode, 1979; Chen & Bode, 1983; Fujinaga et al., 1987; Frigerio et al., 1992), it is clear that the size of the serpins suggests extended interactions with the protease. Interestingly, the eglin C reactive loop is distant from the core and its conformation is maintained through several charged-charged interactions. This situation is similar to the one expected for a serpin.

We built a model for the complex between ACT and PSA. In our serpin model, the reactive loop, from residue P2 to P'2, was forced to adopt a structure similar to the one observed in BPTI, whereas the surrounding residues where allowed to fit the enzyme binding cleft. Exact detail of all the atomic interactions is thus not possible to reproduce, whereas more crude interactions can be detected. In our modeled complexes, the established hydrogen bonding pattern between the backbone atoms P3-P'3 of the inhibitor and the enzyme (Bode & Huber, 1992) was not completely reproduced. At this stage of evaluation, emphasis was on side chain–side chain interactions and overall orientation of the serpins relative to the proteases (Fig. 4).

When building the PSA-ACT complex, the loop 4 of PSA had to be opened manually in order to allow the insertion of the large serpin molecule. This suggests that the original conformation of loop 4 was not optimal, and/or that this loop in fact opens upon binding to a serpin.

Docking thrombin and ACT with the same orientation as in the ACT-PSA complex creates only a few steric clashes with loop 1 of thrombin, but several with loop 5. In thrombin, Trp 148 of loop 5 is too close to antichymotrypsin His 224. This loop is, however, reported to be flexible and can probably open up for such an interaction. Moreover, the reactive loop, from P4 to P'3, would have to be slightly modified to fit properly the active site of thrombin. Loop 2 of thrombin does not have unfavorable contact with our serpin model. Interestingly, all these steric clashes can be avoided easily by manual rotation of some

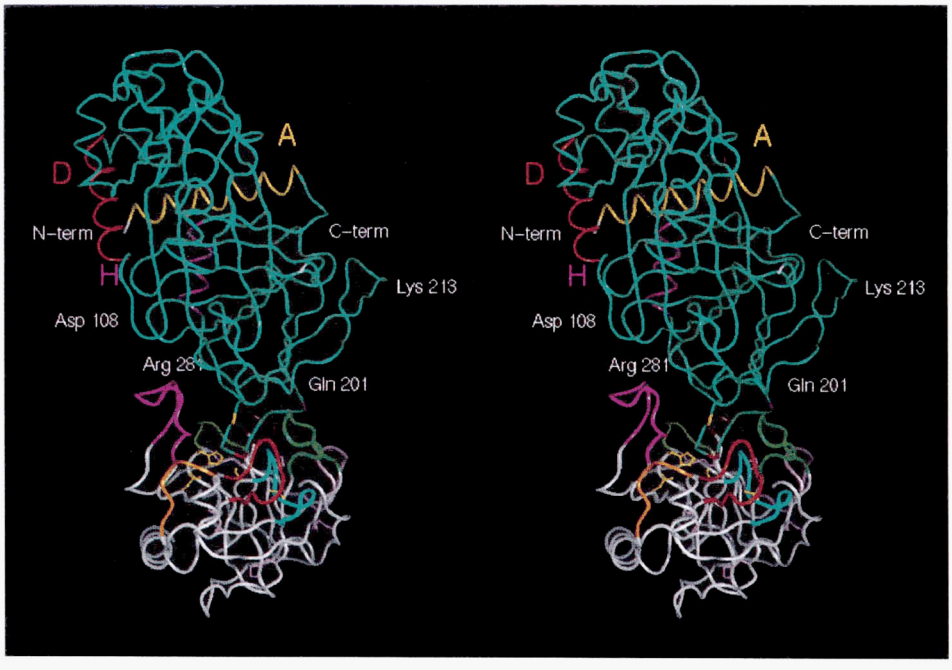

Fig. 4. Interactions between PSA and the core structure of antichymotrypsin. Stereo view of the PSA–antichymotrypsin complex. PSA is in white, but with the loops surrounding the active site colored as in Figure 2. The catalytic triad and S1 residues are displayed in ball and stick representation (yellow). ACT is in blue, the P1 residue is in red, P5 in yellow, and P′5 in magenta. N- and C-terminal residues of ACT are shown in white. Helices A, D, and H are shown in yellow, red, and magenta, respectively.

side chains and energy minimization. All the loops surrounding the active site of thrombin have been suggested to be relatively rigid (Bode et al., 1992), except loop 5. Our thrombin–ACT docking easily accommodated all loops but the flexible loop 5. This suggests that the overall orientation of the serpin relative to the protease is reasonable, because fitting it into the narrow active site cleft of thrombin provides a stringent test.

Projecting the heparin binding residues of thrombin and antithrombin onto PSA and ACT produces a contiguous area on the complex surface. This suggests again that the orientation of PSA in complex with ACT is reasonable.

None of the known or suggested glycosylation sites of ACT (Baumann et al., 1991) seem involved in a contact with PSA in the modeled complex. The closest hypothetical glycosylation site on ACT (Asn 247) is at about 14 Å from the tip of PSA loop 4.

Possible interactions between PSA/hK2 and ACT

The suggested residues involved in the interactions of PSA and hK2 with (1) the serpin reactive loop, residues P5 to P′7, and (2) the serpin core, are given below. It is important to remember that alterations of interprotein orientation may add or remove contacts. To some extent, such different "orientations" have been taken into account in the following. Moreover, there is no experimental evidence yet whether or not hK2 interacts with ACT.

Residues directly in contact with the reactive loop

Before residue P5, no contact between the serpin and the PSA/hK2 enzymes is observed in the models.

Residue Lys 354 (**P5**) of antichymotrypsin points in the direction of PSA Pro 173 [165, loop 6]. The P5 side chain is repelled by PSA Arg 224 [215, loop 8], the side chain of which is only 6 Å away. Lys 354 could interact with the carbonyl backbone atom of PSA Pro 173 [165]. The N_ζ atom of Lys 354 is about 6 Å from the carboxyl group of PSA Gln 174 [166, loop 6] and could be hydrogen bonded to it if the side chains were modified and/or the orientation between the two proteins slightly tilted. In the case of hK2, Pro 173 [165] is a serine and could interact favorably with Lys 354 (P5), because the distance between the N_ζ and O_γ atoms is 3.9 Å. Interestingly, the positive charge is conserved at position 224 [215], because hK2 has a Lys here. In addition, hK2 has a glutamate residue instead of a Gln at position 174 [166], which also could interact with Lys 354. It is important to note that, upon formation of the complex, Glu 218 [208, loop 8] in both hK2 and PSA was pushed slightly inside the enzyme cleft and that an opening of this part of the loop is also possible. In this case, the carboxyl group of this glutamate could interact with Lys 354. In hK2, also Asp 96 [90] and Glu 97 [91] are close to P5, making this part of the molecule negatively charged.

Residue Ile 355 (**P4**) of ACT points toward the serpin core. It does not seem to have specific interaction with the enzyme, although in a different conformation, Pro 95k [89] of loop 4 in PSA or hK2 could interact with P4. In the present model, it has van der Waals contact with the side chain of His 225 (ACT core), possibly helping to maintain the reactive loop in an appropriate conformation. Asp 97 [91] of PSA and Glu 97 [91] of hK2 may interact with the backbone atoms of P5 or P4.

Residue Thr 356 (**P3**) of ACT may interact with PSA residues His 172 [164] and/or Trp 215 [205]. His 172 [164] is a Tyr in hK2

and the Trp is conserved. The Thr 356 O_γ atom could also interact with Gln 174 [166] of PSA and hK2 Glu 174 [166] or with hK2 Glu 96 [91].

Leu 357 (**P2**) of ACT probably interacts with the His 57 [41] imidazole group and possibly with Trp 215 [205] of PSA and hK2. Note that the conserved Ser 99 [93] and Asp 97 [91] (Glu in hK2) in the proteases are close to the P2 residue.

Leu 358 (**P1**) of ACT fits well in the specificity pocket of PSA. In hK2, the nearby S1 Asp 189 [183] makes this hydrophobic P1 residue nonoptimal. Five of these proteases have a large residue at position 192 [186], Met, Glu, or Gln. This residue is expected to block the access of the specificity pocket. In PSA, hK2, and tonin, the corresponding residue has a small side chain (Fig. 1). It is possible in PSA and hK2 that residue Glu 218 [208] plays the role of residue 192 regarding the access to the specificity pocket (Fig. 1).

Ser 359 (**P'1**) of ACT interacts with His 57 [41] of PSA and hK2. In hK2, His 41 [25] can be at hydrogen bonding distance to the P'1 residue. In both enzymes, P'1 is in direct vicinity of the disulfide bridge involving Cys 42 [26] and Cys 58 [42].

Ala 359a (**P'2**) of ACT interacts well with Phe 149 [141] of both PSA and hK2.

Leu 359b (**P'3**) of ACT could interact with Val 41 [25] of PSA, which is a His in hK2. It is also possible that P'3 interacts with the carbon side chain of Arg 39 [23] in PSA. This Arg is a Trp in hK2 and could form a favorable hydrophobic interaction with P'3. It is interesting to note that the P'3 residue tends to point more toward the serpin core than toward the protease, and thus may contribute to the stabilization of the reactive loop. In kallikrein complexed with BPTI (Chen & Bode, 1983), the P'3 residue lies in a very different position compared to our ACT-PSA model. This seems to be the result of the much larger molecular size of the serpins, leading to a flatter overall shape of the reactive loop.

Val 359c (**P'4**) of ACT can interact with Phe 149 [141] of PSA and hK2, and possibly with Phe 74 [57]. At about 4 Å from P'4 are Thr 151 [143] in PSA (Arg in hK2) and Ala 40 [24] (conserved in both enzymes), both of which could interact with P'4. Due to its location, Arg 151 [143] in hK2 probably plays a role for the interaction with the macromolecular substrate/inhibitor. Almost on the opposite side of hK2 Arg 151 [143] lies the side chain of Trp 39 [23], which interacts with P'4. These two large residues are striking when compared to PSA. A different conformation for the reactive loop may bring P'4 closer to the protease residue 39.

The P'4 residue corresponds to Glu 350 of plasminogen activator inhibitor-1 (PAI-1), suggested by Madison et al. (1989, 1990) to interact with Arg 304 of tissue-type plasminogen activator (t-PA), equivalent to Arg 39 [23] of PSA. This is not conserved in our model structures, probably due to the fact that t-PA has an insertion of six residues compared to PSA or hK2 in this region of the enzyme, which probably leads to a different conformation of the reactive loop and/or different orientation of the protease relative to the serpin molecule.

Glu 359d (**P'5**) of ACT interacts with Lys 153 [145] of PSA, which is an Arg in hK2. The carbon atoms of the side chain of the P'5 residue interact also with Phe 74 [57] of PSA and hK2. A different conformation of the reactive loop may bring the P'5 residue into contact with Arg 39 [23] of PSA. This also applies to Trp 39 [23] of hK2 if another rotamer is chosen for this side chain. Two other side chains in hK2 may play a role here; Arg 82 [65], which is a Val in PSA (far from P'5 in PSA), and Arg 70 [53], conserved in PSA.

Thr 360 (**P'6**) of ACT interacts with Arg 39 [23] of PSA, although some ambiguity remains. Depending on the structure of the reactive loop and loop 1 of the enzyme, P'6 may have little interaction with the proteases. P'6 does not seem to interact with hK2.

Arg 361 (**P'7**) points toward the core of ACT and does not seem to interact with the enzyme. In the model, P'7 is involved in a salt bridge with Glu 285, and thus appears to stabilize the reactive loop structure. P'7 may be in contact with Glu 148 [140] of PSA and hK2, but the orientation of its side chain is ambiguous.

It interesting to note that many of the interactions mentioned above correlate well with a recent paper by Cooper et al. (1995).

Protease residues possibly in contact with the core of the serpin molecules

Loop 1 (35 [20]–41 [25]) and 2 (59 [43]–64 [48]). In the PSA-ACT model complex, PSA Ser 35 [20] can interact with ACT residue Glu 282. This glutamic acid seems also to be involved in a salt bridge with PSA Arg 60 [44]. In the case of hK2, Ser 35 [20] is conserved and Arg 60 [44] is replaced by a Lys and thus these two residues could interact with Glu 282 of ACT. It is also possible that Arg 60 [44] in PSA and Lys 60 [44] of hK2 make a hydrogen bond with Thr 226a of ACT, which is close to Glu 282 in the three-dimensional structure.

Loop 4 (95a [79]–98 [92]). PSA/hK2 residues Leu 95c [81] and Leu 95d [82] may interact with Phe 280 of ACT. Lys 95e [83] in PSA/hK2 interacts with Glu 195 of ACT. Depending on the structure of loop 4, Arg 95g [85] could interact with Glu 195 of ACT, whereas in our model, this Arg residue points outward. Arg 95j [88] in PSA and hK2 forms a salt bridge with Glu 109 of ACT. It is also possible that some of these charged residues in PSA and hK2 interact with backbone atoms in these areas of ACT, instead of the side chains noted above.

Loop 5 (142 [134]–153 [145]) and loop 8 (residue 216 [206]–226 [217]). Glu 147 [139] of PSA can interact with ACT His 224 or Gln 201. Glu 148 [140] of PSA can interact with His 224 of ACT or with Arg 361 if the latter is extended and oriented toward loop 5. It is also possible that PSA Glu 148 [140] interacts with Tyr 287 of ACT if loop 5 opens up slightly. Although His 204, 224, and 225 of ACT are in the vicinity of the two glutamates of PSA, it is interesting to note that this area of ACT has also several negative charges not expected for an optimal contact, unless they modulate the interaction of the two molecules. The negative charges in this part of ACT are Glu 285, Asp 202, and Asp 199. Also, in close vicinity of PSA Glu 147 [139] is Glu 218 [208] at the tip of loop 8. This Glu 218 [208] seems to interact with His 225 of ACT, although opening of the loop may bring it into contact with Lys 354 (P5 residue) of the reactive loop. These interactions are also relevant for hK2 as Glu 147 [139], 148 [140], and 218 [208] are conserved.

Electrostatics potential analysis

The role of electrostatic interactions for protein stability and protein substrate/inhibitor binding is evident (Warshel & Åqvist, 1991; Bashford & Gerwert, 1992; Karshikov et al., 1992; Honig & Nicholls, 1995).

In this article, we computed the electrostatics data using the Finite Difference method to solve the Poisson-Boltzmann equation, whereas pH-dependent calculations (Spassov et al., 1989; Villoutreix et al., 1994b) of the different proteins are in progress. In the following paragraphs, we compare some of the electrostatic properties of (1) PSA and hK2, (2) cleaved and uncleaved ACT, and (3) the PSA-ACT complex. In the latter, the discussion will be extended briefly to include the putative hK2-ACT complex.

Electrostatic potential comparison of PSA and hK2

With the set of charges used, PSA has a net charge of +5.5e, whereas the total charge for hK2 was +3e. In observing the binding site area (Fig. 5A), the active site cleft of PSA is mainly of negative potential at the energy level plotted (±1 kcal/mol [≅ ±1.7 kT/e]), whereas the loops surrounding the active site mostly display positive potential. This character is similar in hK2, although a more pronounced dipole-like pattern is observed in the active site area. The loops of domain B in hK2 are less positive than in PSA (Fig. 5A).

In PSA, loops 1, 2, 3, the tip of loop 4, a stretch around residue 152 [144] of loop 5, a stretch around residue 215 [205] of loop 8, a stretch around residue 187 [180], the tip of loop 7, a stretch around residue 172 [164] of loop 6, and most of the side opposite to the binding site are mainly within the positive isopotential. From the active site cleft, the negative surfaces protrude out of the molecule. Loop 5, the base of loop 4 (toward the active site area), the catalytic triad, and part of the specificity pocket (including Ser 189 [183]) are mainly enclosed in the negative isopotential. hK2 lacks the neutral area found in PSA between loops 1 and 2 and the active site cleft (Fig. 5A).

Most of the differences between the electrostatic surfaces of these two proteins are not computationally significant, particularly on the back side of the molecules.

Electrostatic potential comparison of cleaved and uncleaved ACT

The total charge obtained for the uncleaved antichymotrypsin was −3.5e. When comparing the isopotential surfaces between cleaved and uncleaved ACT, the most interesting differences was the slight enhancement of the positive contour in an area between the reactive loop and the core of the protein (Fig. 5B). It is also interesting to note a change in the positive potential in the areas of helices A, B, and D. The distribution of the potential isosurfaces is mosaic, whereas a positive area partially covers sheet A. As a comparison, similar computations were performed on the uncleaved form of a PCI model (B.O. Villoutreix, unpubl. data). Uncleaved PCI has a net charge of +13.5e when including the N-terminus A+ helix (Kuhn et al., 1990) residues. As expected for a protein with such a positive net charge, PCI is mainly covered by a positive potential with small areas of negative potential distributed mainly in the region opposite to the reactive loop (see Radtke et al., 1995 for computations conducted on a cleaved PCI model). These electrostatic differences should play a role in the PSA–serpin complexes formation.

Electrostatic contour complementarities between PSA and ACT

The area around residues Arg 281 or Tyr 229 of ACT (above PSA loops 1 and 2) shows a positive contour covered by a negative one that extends outside the molecule toward ACT Pro 228 and Asp 108 (just above loop 4 of PSA in the orientation of Fig. 4). The area above the "positive" domain A of PSA is mainly negative in ACT. This produces favorable electrostatic overlaps between the two molecules (Fig. 5B).

Above the tip of PSA loop 5 and the region of loop 8, ACT also exhibits negative surfaces. These surfaces in ACT enclose the region between Gln 201 and Val 353 (the P4 residue) and cover part of the core structure above this area. In the PSA region below ACT residue Gln 201, negative surfaces protrude from the molecule and overlap with the negative surfaces of ACT. From the ACT sheet C, behind the reactive loop, toward the core of the molecule (region of residues Gln 205 and Trp 215 of ACT), lies an area of positive surfaces. These positive surfaces overlap favorably with negative surfaces surrounding the tip of loop 5 in PSA and within the active site cleft area (Fig. 5A,B).

The analysis of the electrostatic complementarities between PSA-ACT complexes are similar for hK2 in spite of minor differences.

Suggested PSA heparin binding sites

Complex formation between thrombin and antithrombin or protein C and protein C inhibitor is enhanced significantly by heparin (Jordan et al., 1980; Suzuki et al., 1983). We reported that complex formation between PSA and PCI is enhanced about sixfold in the presence of heparin (Christensson & Lilja, 1994), whereas the opposite effect is observed in the presence of heparin when the complex PSA-ACT is studied (H. Lilja, unpubl. data).

The protease domains

Many of the heparin-binding residues are known in the case of thrombin. These include mainly Arg 93, 97, 101, 126, 165, 173, 175 and Lys 169, 236, and 240 (Fig. 1) (Bode et al., 1992; Schreuder et al., 1994; Sheehan & Sadler, 1995). In thrombin, these residues are mainly situated around loop 4, loop 6, and the C-terminal helix, and thus correspond roughly to one side of the protease domain A. Projecting these residues onto PSA indicates that many of them are not conserved (2 of 10). However, PSA exhibits two areas with positively charged residues not counter-balanced by negative charges and where heparin could bind. One area differs from that expected from thrombin and the other is relatively similar. In the area surrounding the binding site of PSA, loops 1 and 2 have a cluster of four positively charged residues (Arg 36 [21], 39 [23], 60 [44], and Lys 62 [46]). This area could extend toward the C-terminal helix or even toward Lys 153 [145] and 154 [146] (end of loop 5). This part of PSA is, however, glycosylated at Asn 61 [45], and it is not known whether the sugar molecule affects heparin binding. The other area in PSA that is a candidate for heparin binding includes loop 4, loop 6, and possibly extends to the C-terminal helix. This area would resemble the anion binding exosite II of thrombin. Three positively charged residues are present on loop 4, Lys 95e [83], Arg 95g [85], and 95j [88]. Loop 6 provides two further positively charged residues, 175 [167] and 178 [170]. Finally, the area of the C-terminal helix contains Lys 230 [221], 236 [227], and 239 [230], and Arg 235 [226]. The positive residues in these two areas of PSA give in part rise to the positive aspect of the electrostatic potential surfaces described above. In hK2, many of the positively charged residues are conserved in

A

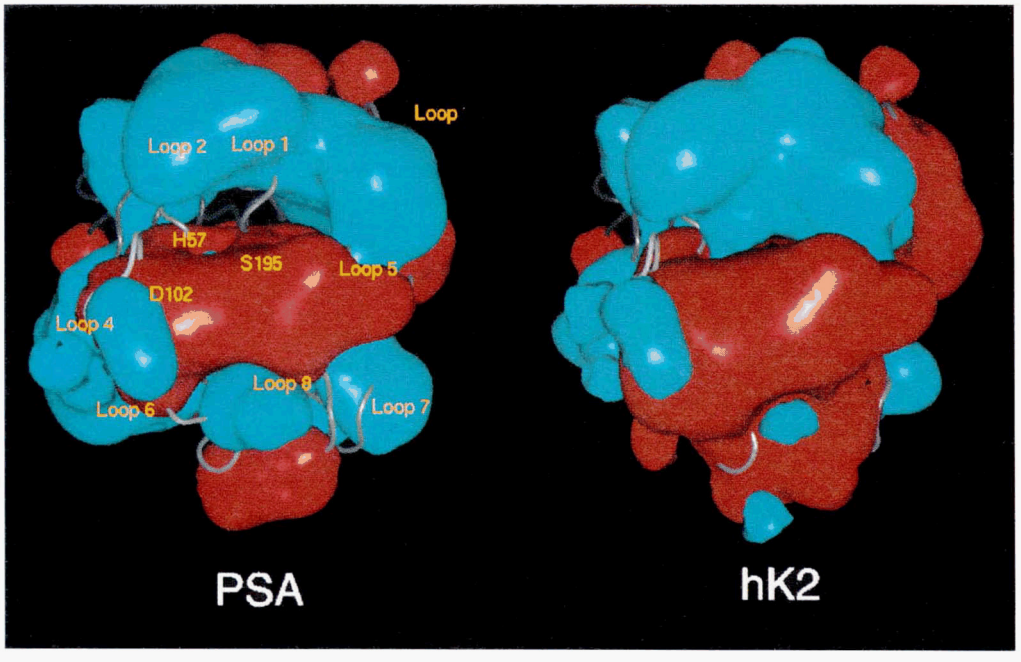
Loop
Loop 2
Loop 1
H57
S195
Loop 5
D102
Loop 4
Loop 8
Loop 6
Loop 7
PSA
hK2

B

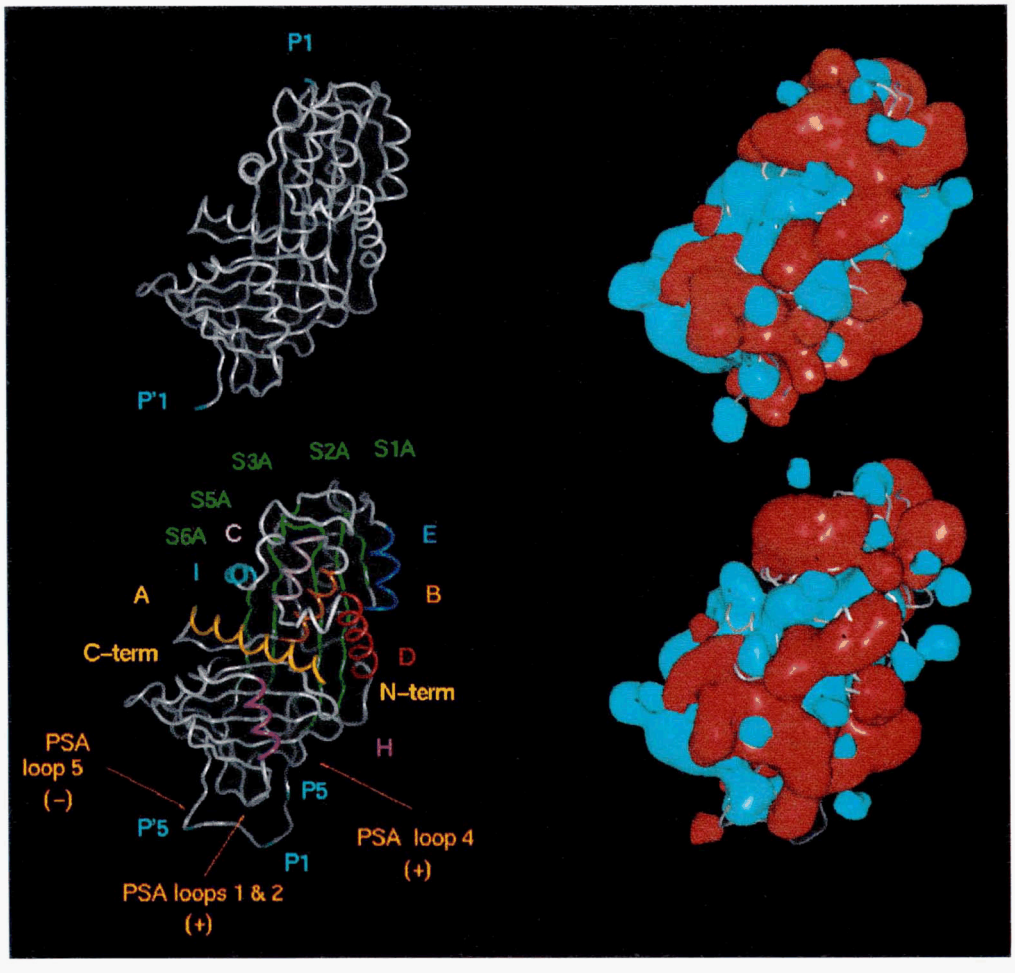
P1
P'1
S3A
S2A
S1A
S5A
S6A
C
E
I
A
B
C-term
D
N-term
H
PSA
loop 5
(-)
P5
P'5
PSA loop 4
(+)
P1
PSA loops 1 & 2
(+)

the C-terminal helix, whereas several are missing from loops 1, 2, or 4 (Fig. 1). When comparing PSA and hK2 positive electrostatic surfaces to seek potential heparin binding sites, it is seen that PSA has a more pronounced positive area at the base (to the extreme left in Fig. 5A) and tip of loop 4, around the C-terminal helix, and around loops 1 and 2. These positive surfaces in PSA are more outside of the molecule, whereas they are more pronounced inside the binding site cleft in hK2.

Because the interaction of activated protein C (APC) with PCI is also enhanced by heparin, it was interesting to perform a similar analysis on an APC model (Fisher et al., 1994) and compare the results with the one observed for PSA. In protein C, loops 1, 2, 3, and 5, as well as the region below loop 3 (region N-terminal to the activation site of PC, residues 141–169), are rich in positively charged residues and are enclosed in positive isosurfaces (data not shown). These regions differ significantly from what is observed in thrombin (Greengard et al., 1994). Protein C has a net charge of +7e (depending on the model used) and has its binding cleft largely enclosed in a negative potential. Two main areas of positive potential are seen, one running from the end of the C-terminal helix to behind loop 3, and the other surrounding loop 5. Interestingly, the positive surfaces in protein C protrude significantly outside the surface of the molecule. If heparin binds protein C in an area behind loops 1, 2, 3, or in the vicinity of loop 5, the number of positively charged residues is much higher than in PSA. The binding of heparin to APC would therefore be much stronger than the one observed for PSA. This could explain in part why heparin significantly enhances the complex formation between APC and PCI (heparin compensates unfavorable positive potential overlaps, see below), whereas the increase is only sixfold in the case of PSA-PCI.

The results of our structural and electrostatic analysis with regard to the protein C putative heparin-binding site are in good agreement with the suggestion made by Cooper et al. (1995).

The serpin molecules

In antithrombin, the main residues involved in heparin binding are Arg 46, 47, 129, 132 and Lys 107, 114, 125, 133, and 136 (Huber & Carrell, 1989; Schreuder et al., 1994). This area corresponds mainly to the A and D helices of antithrombin (Figs. 3, 5B). This area of antithrombin is above loops 4, 6, and the C-terminal helix area of PSA (in the orientation of Fig. 4). The corresponding area in antichymotrypsin is much less positive (Fig. 5B). The A+ helix of PCI lies in an area that contains a cluster of positively charged residues (Kuhn et al., 1990). The helix D of PCI is less positively charged than in antithrombin, and thus it was suggested that helix H could be involved in heparin binding instead (Kuhn et al., 1990; Shirk et al., 1994). The region surrounding this helix also contains several positive residues.

The heparin binding sites

In the area above loops 1 and 2 in a PSA-PCI complex (B.O. Villoutreix, unpubl. data), the PCI molecule possesses several positively charged residues. These are: Arg 366, Arg 282, Lys 280, and more distantly, Arg 233, Lys 274, Lys 277, Lys 274, Lys 270 (mainly H helix), and Arg 10, Lys 14, Arg 15 (A+ helix). This suggests that heparin may bind to PCI along these two helices and reach PSA either at loops 1 and 2 or at loop 4, and eventually extend to the C-terminal helix of PSA or toward the end of loop 5 in the B domain. These observations could hold for protein C.

In ACT, the area of the H helix and below (toward the reactive loop) contains only few positively charged residues and has negative residues instead, such as Glu 241, Asp 277, Glu 279, and Glu 282 above loop 1 and 2, and Glu 195, Asp 108, and Glu 109 above PSA loop 4 (Fig. 5B). The binding of heparin to PSA either in the region of loop 4 or close to loops 1 and 2 would place the negatively charged glycosaminoglycan molecule in unfavorable contact with the negatively charged residues of ACT (Fig. 5B).

As a whole, the electrostatic observations for the model complexes seem to be supported by experimental results and suggest that the overall orientation between the proteases and the serpin molecules is valid.

Conclusion

PSA and hK2 are expected to share significant structural similarities based upon the model-building experiments. No striking differences are detected regarding accessible hydrophobic clusters or electrostatic isopotential contours. Because amino acid substitutions are mainly located in the loops surrounding the binding sites, it can be suggested that these two proteins probably have different substrates or inhibitors. This result is highlighted by the fact that the S1 residue of PSA is a Ser, whereas the corresponding residue of hK2 is an Asp. It seems likely that the uncleaved ACT adopts a structure similar to the one observed for antithrombin. Due to the electrostatic complementarities and the data observed for heparin, we suggest that the orientation of the serpin molecule relative to the protease model is realistic. Numerous side-chain–side-chain interactions are reported between PSA and ACT. These observations are extended to hK2 and can be adapted to PSA/hK2-PCI complexes based upon the sequence alignment tables. Although these interactions have to be taken with caution, our results help to de-

Fig. 5. Electrostatic surface potential of PSA, hK2, and ACT. **A:** Comparison of PSA and hK2. PSA and hK2 are represented in the same orientation as is PSA in Figure 2. The isopotential contours for PSA and hK2 are shown at −1 kcal/mol (red) and +1 kcal/mol (blue) [$\cong \pm 1.7\ kT/e$]. The loops and the catalytic triad residues are labeled in yellow on the PSA model structure. Electrostatic surfaces are relatively similar between the two molecules. **B:** Comparison between cleaved and uncleaved ACT. Cleaved and uncleaved ACT are shown in a white ribbon representation on the left side of the figure. In the same orientation are shown the isopotential contours at an energy level of −1 kcal/mol (red) and +1 kcal/mol. The P5, P1, P′1, P′5 residues are shown in blue. Some of the loops of PSA expected to be in close contact with ACT are also indicated. The C- and N-terminal regions of the ACT model are labeled and shown in yellow. The sheet A is in green and some of the helices are colored and labeled (i.e., the helix A is in yellow and the upper case letter "A" is shown in yellow).

sign synthetic peptide antibodies and "rational" site-directed mutagenesis experiments on PSA, hK2, APC, PCI, and ACT.

Materials and methods

Construction of the PSA and hK2 models

The X-ray structures of rat tonin (entry 1TON) (Fujinaga & James, 1987), porcine kallikrein (entry 2PKA) (Bode et al., 1983), bovine trypsin (entry 1TLD) (Bartunik et al., 1989), bovine chymotrypsin (entry 5CHA) (Blevins & Tulinsky, 1985), human thrombin (entry 1TMT) (Bode et al., 1989), and a recently developed model for the human natural anticoagulant protein C (entry 1PCU) (Fisher et al., 1994) were superimposed. Energy-minimized PSA models were obtained from Villoutreix et al. (1994a).

Briefly, the PSA models were built using the atomic coordinates of kallikrein (Bode et al., 1983) and tonin (Fujinaga & James, 1987). The loop 4 of PSA was 7–8 residues longer when compared to these two X-ray template structures (Fig. 1). This loop 4 was generated using the random tweak algorithm (Shenkin et al., 1987) and simulated in vacuo using high-temperature molecular dynamics and annealing (Villoutreix et al., 1994a). Several conformations for loop 4 were used initially and tested as to whether they allow the docking of the uncleaved ACT model into the active site of PSA. hK2 was built using a selected PSA model and the X-ray structure of kallikrein.

Structural and sequence alignment of ACT

The atomic coordinates of uncleaved human antithrombin (ATIII) (entry 1ATH; Schreuder et al., 1994), cleaved human protein C inhibitor (PCI) model structure (entry 1PAI; Kuhn et al., 1990), cleaved human α_1-antitrypsin (AT) (entry 7API; Loebermann et al., 1984), and α_1-antichymotrypsin (ACT) (entry 2ACH; Baumann et al., 1991) were obtained from the Protein Data Bank (Bernstein et al., 1977). The four structures were superimposed using the Homology software (Biosym Technologies, Inc). The location of secondary structure elements in ATIII and information obtained from the structural alignment were used to align the sequences. Further manual modifications in the alignment were added according to Huber and Carrell (1989) and the final alignment is reported in Figure 3. Because the main goal was to model the reactive loop region, the only insertion of interest was the addition of Thr 360 in ACT as compared with the sequence of ATIII. Different sequence alignments are possible around Thr 360 of ACT. Here we built the Thr as an insertion when compared to ATIII and the subsequent Arg of ACT was assumed to match the Arg of ATIII (Fig. 3). Thus, Arg 361 in ACT points into the space between the reactive loop and the core of the protein and presumably contributes to the stabilization of the loop. Other alternatives are conceivable for this residue.

Construction of the uncleaved ACT model

The model was constructed from the atomic coordinates of the cleaved ACT and the uncleaved ATIII with the programs Quanta (Molecular Simulation Inc.), and Homology (Biosym Technologies, Inc.).

The strand 4A (Fig. 3) of the cleaved ACT was removed and replaced by the corresponding residues of the reactive loop of ATIII. When present, values for the side-chain torsion angles (χ) in ATIII were used for each substitution. When the side chains were longer in ACT than the ATIII side chains, an extended conformation was used for the remaining χ angles initially. A rotamer library (Ponder & Richards, 1987) was then used to optimize the orientation of the new side chains.

The Thr 360 insertion in ACT was constructed by means of the program Homology using the random tweak algorithm. This generates a loop de novo by randomly searching the conformational space for a suitable backbone conformation, whereas steric overlaps and a set of distances between two anchor residues (Val 359c and Thr 362 in ACT) are taken into account (Shenkin et al., 1987). Two-hundred cycles of steepest-descent energy minimization were performed using the simulation program Discover (Biosym Technologies, Inc.) on the newly built loop in order to optimize the peptide bonds and side-chain geometry, whereas the rest of the ACT structure was held fixed.

Energy minimization of ACT

No severe overlaps between atoms were detected during the construction of the uncleaved ACT model. The minor steric clashes and bond strain due to the building of the reactive loop were regularized using Discover (Biosym Technologies, Inc.) and the corresponding CVFF force field parameters (Hagler et al., 1974; Hagler & Lifson, 1974). Hydrogen atoms were added to the model structure according to standard geometries. Refinement of the structure was conducted in stages. The first step involved several cycles of steepest-descent energy minimization without any constraining forces (because no major structural modifications were noticed on a test model) and minimized until the maximum Cartesian derivative was less than 50 kcal/mol/Å. The second step involved the minimization of only the sheet A, helix F, and the subsequent region (from helix F to the strand S3A). The hydrogen bond pattern of the ATIII sheet A (Schreuder et al., 1994) was partly reproduced by 500 cycles of steepest-descent minimization with restraints. Additional minimization was performed until the maximum derivative was less than 5 kcal/mol/Å using the steepest-descent algorithm. Finally, the minimization was continued until the maximum derivative was less than 1 kcal/mol/Å using conjugate gradients. All calculations were performed using a 20-Å nonbond cutoff, a dielectric permittivity of 1, harmonic bond and bond angle potentials, and neglecting cross terms.

Finally, a 5-ps molecular dynamics simulation at room temperature was performed on the sheet A and helix F regions to further refine this area of the ACT molecule while keeping the rest of the structure fixed.

The reactive loop of the ACT model

The reactive loop of ATIII is inserted partially into the central sheet A. Such a conformation may facilitate the subsequent incorporation of the N-terminal portion of the reactive loop into the β-sheet A upon proteolytic cleavage of the serpin (Bode & Huber, 1991; Katz & Christianson, 1993). Thus, the reactive loop in ATIII should accurately represent an uncleaved serpin in an inhibitory conformation. However, in this X-ray structure, the residue Arg 393 (the P1 residue for thrombin) points inward.

This seems to be the result of the dimeric structure present in the crystal rather than an appropriate conformation to interact with a serine protease (Schreuder et al., 1994). Therefore, in order to modify this region of the reactive loop, we (1) docked a four-residue peptide into the active site of PSA and (2) energy minimized the reactive loop of the ACT model with restraints on the ψ, ϕ, and χ angles in order to match the ones observed for the short peptide.

Ligand docking in the PSA active site

A short peptide from the reactive loop of ACT (sequence = $LL_{pI}SA$) was first positioned into the active site of PSA using the kallikrein:bovine pancreatic trypsin inhibitor complex as template (Chen & Bode, 1983). As already pointed out by Greer (1981) and Bode et al. (1992), the serine protease inhibitors have a highly conserved structure for the backbone atoms between residues P2 and P'2 and start to differ after residue P3 and P'3. Therefore, only residues P2–P'2 of BPTI were selected and computationally mutated to the corresponding sequence of ACT. A short energy minimization (200 cycles of steepest descent with a tethered force constant of 20 kcal/mol/Å^2 on all the heavy atoms) was performed on the PSA model complexed with the peptide structure.

Energy minimization of the reactive loop of ACT

The list of angles obtained from the peptide structure (P2–P'2) were used to force the corresponding residues in the reactive loop of the ACT model to adopt the canonical structure of the serine protease inhibitor (Bode et al., 1992). The backbone of residues P6–P3 and P'3–P'6 modeled according to ATIII were tethered to their position with a force constant of 20 kcal/mol/Å^2, whereas the rest of the structure was fixed. The structure was energy minimized for 200 cycles of steepest descent. No further refinement of the loop was performed prior to docking the two models.

Modeling the ACT:PSA complex

The ACT model was docked manually into the active site of PSA, using the docked peptide as initial guideline. Only few residues of loop 4 of the selected PSA model produced steric clashes with the ACT, thus the loop was modified interactively first and optimized by brief energy minimization. Subsequently, a few side chains of the PSA and ACT models were modified manually or by using a rotamer library (Ponder & Richards, 1987) in order to remove steric clashes. The complex was then energy minimized again by 200 cycles of steepest descent and 200 cycles of conjugate gradient. Because several ω angles in the kallikrein loop of PSA (loop 4) were still problematic due to manual opening of the loop, it then seemed appropriate to rebuild loop 4 using the random tweak algorithm, while taking into account the presence of the ACT structure. A loop conformation that did not present unfavorable steric clashes with the serpin molecule was selected and further refined by energy minimization within the PSA-ACT complex.

Electrostatic calculations

The finite difference Poisson Boltzmann (FDPB) method (Klapper et al., 1986; Gilson et al., 1987; Sharp & Honig, 1990) was used to calculate the three-dimensional distribution of the electrostatic potential. The FDPB was solved with the program DelPhi (Biosym Technologies, Inc.). The protein atomic coordinates were mapped onto a cubic three-dimensional grid of $65 \times 65 \times 65$ at a spacing of 1 Å, with a distance of 10 Å between the protein surface and the grid edge. The ionic strength was set to 0.1 M and the dielectric constant to 4 in the protein interior and 80 in the surrounding solvent (Harvey, 1989). Atomic radii were assigned using DelPhi default parameters with the radii of hydrogen atoms set to 0 Å. The standard set of formal charges were assigned to the ionized groups (−1 for Asp and Glu, +1 for Lys and Arg, and 0.5 for His). The resulting three-dimensional electrostatic maps were analyzed with the graphics program Insight II (Biosym Technologies, Inc.).

Calculation of solvent accessibilities

The normalized static solvent accessibilities were calculated according to Lee and Richards (1971). All side chains with a surface accessibility less than 0.20 Å^2 were considered to be internal, although the titratable part sometimes may be partially or fully solvent accessible.

Acknowledgments

We acknowledge a grant by the Academy of Finland, the Swedish Medical Research Council (project no. 7903), and the Swedish Cancer Society (project no. 3555).

References

Akiyama K, Nakamura T, Iwanaga S, Hara M. 1987. The chymotrypsin-like activity of human prostate-specific antigen, γ-seminoprotein. *FEBS Lett 225*:168–172.

Bartunik HD, Summers LJ, Bartsch HH. 1989. Crystal structure of bovine β-trypsin at 1.5 Å resolution in a crystal form with low molecular packing density. Active site geometry, ion pairs and solvent structure. *J Mol Biol 210*:813–828.

Bashford D, Gerwert K. 1992. Electrostatic calculations of the pK_a values of ionizable groups in bacteriorhodopsin. *J Mol Biol 224*:473–486.

Baumann U, Huber R, Bode W, Grosse D, Lesjak M, Laurell CB. 1991. Crystal structure of cleaved α_1-antichymotrypsin at 2.7 Å resolution. *J Mol Biol 218*:595–606.

Bélanger A, van Halbeek H, Graves HCB, Granbois K, Stamey TA, Huang L, Poppe I, Labrie F. 1995. Molecular mass and carbohydrate structure of prostate specific antigen: Studies for the establishment of an international PSA standard. *The Prostate 27*:187–197.

Bernstein FC, Koetzle TF, Williams GJB, Meyer EF Jr, Brice MD, Rodgers JR, Kennard O, Shimanouchi T, Tasmui M. 1977. The Protein Data Bank: A computer-based archival file for macro-molecular structures. *J Mol Biol 112*:535–542.

Blevins RA, Tulinsky A. 1985. The refinement and the structure of the dimer of α-chymotrypsin at 1.67 Å resolution. *J Biol Chem 260*:4264–4275.

Blundell TL, Sibanda BL, Sternberg MJE, Thornton JM. 1987. Knowledge-based prediction of protein structures and design of novel molecule. *Nature 326*:347–352.

Bode W. 1979. The transition of bovine trypsinogen to a trypsin-like state upon strong ligand binding. *J Mol Biol 127*:357–374.

Bode W, Chen Z, Bartels K, Kutzbach C, Schmidt-Kastner G, Bartunik H. 1983. Refined 2 Å X-ray crystal structure of porcine pancreatic kallikrein A, a specific trypsin-like serine proteinase. *J Mol Biol 164*:237–282.

Bode W, Huber R. 1991. Ligand binding: Proteinase–protein inhibitor interactions. *Curr Opin Struct Biol 1*:45–52.

Bode W, Huber R. 1992. Natural protein proteinase inhibitors and their interaction with proteinases. *Eur J Biochem 204*:433–451.

Bode W, Mayr I, Baumann U, Huber R, Stone SR, Hofsteenge J. 1989. The refined 1.9 Å crystal structure of human α-thrombin: Interactions with D-Phe-Pro-Arg chloromethylketone and significance of the Tyr-Pro-Pro-Trp insertion segment. *EMBO J 8*:3467–3475.

Bode W, Turk D, Karshikov A. 1992. The refined 1.9 Å X-ray structure of

D-Phe-Pro-Arg chloromethylketone-inhibited human α-thrombin. *Protein Sci 1*:426–471.
Bridon DP, Dowell BL. 1995. Structural comparison of prostate-specific antigen and human glandular kallikrein using molecular modeling. *Urology 45*:801–806.
Brillard-Bourdet M, Moreau T, Gauthier F. 1995. Substrate specificity of tissue kallikreins: Importance of an extended interaction site. *Biochim Biophys Acta 1246*:47–52.
Carrell RW, Stein PE, Fermi G, Wardell MR. 1994. Biological implications of a 3 Å structure of dimeric antithrombin. *Structure 2*:257–270.
Chen Z, Bode W. 1983. Refined 2.5 Å X-ray crystal structure of the complex formed by porcine kallikrein A and the bovine pancreatic trypsin inhibitor. *J Mol Biol 164*:283–311.
Christensson A, Björk T, Nilsson O, Dahlén U, Matikainen MT, Cockett ATK, Abrahamsson PA, Lilja H. 1993. Serum prostate-specific antigen complexed to α_1-antichymotrypsin as an indicator of prostate cancer. *J Urol 150*:100–105.
Christensson A, Laurell CB, Lilja H. 1990. Enzymatic activity of prostate-specific antigen and its reactions with extracellular serine proteinase inhibitors. *Eur J Biochem 194*:755–763.
Christensson A, Lilja H. 1994. Complex formation between protein C inhibitor and prostate specific antigen in vitro and in human plasma. *Eur J Biochem 220*:45–53.
Clements JA, Mukthar A. 1994. Glandular kallikreins and the prostate-specific antigen are expressed in the human endometrium. *J Clin Endocrinol Metab 78*:1536–1539.
Cohen FE, Gregoret LM, Amiri P, Aldape K, Railey J, McKerrow JH. 1991. Arresting tissue invasion of a parasite by protease inhibitors chosen with the aid of computer modeling. *Biochemistry 30*:11221–11229.
Cooper ST, Whinna HC, Jackson TP, Boyd JM, Church FC. 1995. Intermolecular interactions between protein C inhibitor and coagulation proteases. *Biochemistry 34*:12991–12997.
España F, Gilabert J, Estelles A, Romeu A, Aznar J, Cabo A. 1991. Functionally active protein C inhibitor/plasminogen activator inhibitor-3 (PCI/PAI-3) is secreted in seminal vesicles, occurs at high concentrations in human seminal plasma and complexes with prostate-specific antigen. *Thromb Res 64*:309–320.
España F, Sanches-Cuenca J, Vera CD, Estelles A, Gilabert J. 1993. A quantitative ELISA for the measurement of complexes of prostate-specific antigen with protein C inhibitor when using a purified standard. *J Lab Clin Med 122*:711–719.
Fernández JA, Villoutreix BO, Hackeng TM, Griffin JH, Bouma BN. 1994. Analysis of protein S C4b-binding protein interactions by homology modeling and inhibitory antibodies. *Biochemistry 33*:11073–11078.
Fisher CL, Greengard JS, Griffin JH. 1994. Models of the serine protease domain of the human antithrombotic plasma factor activated protein C and its zymogen. *Protein Sci 3*:588–599.
Frigerio F, Coda A, Pugliese C, Lionetti C, Menegatti E, Amiconi G, Schnebli HP, Ascenzi P, Bolognesi M. 1992. Crystal and molecular structure of the bovine α-chymotrypsin-eglin C complex at 2.0 Å resolution. *J Mol Biol 225*:107–123.
Fujinaga M, James MNG. 1987. Rat submaxillary gland serine protease, Tonin, structure solution and refinement at 1.8 Å resolution. *J Mol Biol 195*:373–396.
Fujinaga M, Sielecki AR, Read RJ, Ardelt W, Laskowski M Jr, James MNG. 1987. Crystal and molecular structures of the complex α-chymotrypsin with its inhibitor turkey ovomucoid third domain at 1.8 Å resolution. *J Mol Biol 195*:397–418.
Furie B, Bing DH, Feldmann RJ, Robinson DJ, Burnier JP, Furie BC. 1981. Computer-generated models of blood coagulation factor Xa, factor IXa, and thrombin based upon structural homology with other serine proteases. *J Biol Chem 257*:3875–3882.
Gilson M, Sharp K, Honig B. 1987. Calculating the electrostatic potential for molecules in solution. *J Comput Chem 9*:327–335.
Greengard JS, Fisher CL, Villoutreix B, Griffin JH. 1994. Structural basis for type I and type II deficiencies of antithrombotic plasma protein C: Patterns revealed by three-dimensional molecular modeling of mutations of the protease domain. *Proteins Struct Funct Genet 18*:367–380.
Greer J. 1981. Model of a specific interaction. *J Mol Biol 153*:1043–1053.
Greer J. 1990. Comparative modeling methods: Application to the family of the mammalian serine proteases. *Proteins Struct Funct Genet 7*:317–334.
Hagler AT, Huler E, Lifson S. 1974. Energy functions for peptides and proteins. I. Derivation of a consistent force field including the hydrogen bond from amide crystals. *J Am Chem Soc 96*:5319–5327.
Hagler AT, Lifson S. 1974. Energy functions for peptides and proteins. II. The amide hydrogen bond and calculation of amide crystal properties. *J Am Chem Soc 96*:5327–5335.
Harvey S. 1989. Treatment of electrostatic effects in macromolecular modeling. *Proteins Struct Funct Genet 5*:78–92.
Hedstrom L, Szilagyi L, Rutter WJ. 1992. Converting to chymotrypsin: The role of surface loops. *Science 255*:1249–1253.
Henttu P, Lukkarinen O, Vihko P. 1990. Expression of the gene coding for human prostate-specific antigen and related hGK-1 in benign and malignant tumors of the human prostate. *Int J Cancer 45*:654–660.
Honig B, Nicholls A. 1995. Classical electrostatics in biology and chemistry. *Science 268*:1144–1149.
Huber R, Carrell W. 1989. Implications of the three-dimensional structure of α_1-antitrypsin for structure and functions of serpins. *Biochemistry 28*:8951–8966.
Insight II, DelPhi, Homology, Discover. San Diego, California: Biosym-MSI.
Jordan RE, Oosta GM, Gardner WT, Rosenberg RD. 1980. The kinetics of hemostatic enzyme–antithrombin interactions in the presence of low molecular weight heparin. *J Biol Chem 255*:10081–10090.
Karshikoff A, Bode W, Tulinsky A, Stone SR. 1992. Electrostatic interactions in the association of proteins: An analysis of thrombin–hirudin complex. *Protein Sci 1*:727–735.
Katz DS, Christianson DW. 1993. Modeling the uncleaved serpin antichymotrypsin and its chymotrypsin complex. *Protein Eng 6*:701–709.
Klapper I, Hagstrom R, Fine R, Sharp K, Honig B. 1986. Focusing of electric fields in the active site of Cu-Zn superoxide dismutase: Effects of ionic strength and amino-acid modification. *Proteins Struct Funct Genet 1*:47–59.
Kuhn LA, Griffin JH, Fisher CL, Greengard JS, Bouma BN, Espana F, Tainer JA. 1990. Elucidating the structural chemistry of glycosaminoglycan recognition by protein C inhibitor. *Proc Natl Acad Sci 87*:8506–8510.
Le Bonniec BF, Guinto ER, Stone SR. 1995. Identification of thrombin residues that modulate its interactions with antithrombin III and α1-antitrypsin. *Biochemistry 34*:12241–12248.
Lee B, Richards FM. 1971. The interpretation of protein structure: Estimation of static accessibility. *J Mol Biol 55*:379–400.
Leinonen J, Lövgren T, Vornanen T, Stenman UH. 1993. Double-label time resolved immunofluorometric assay of prostate-specific antigen and its complex with α_1-antichymotrypsin. *Clin Chem 39*:2098–2103.
Lilja H, Abrahamsson PA, Lundwall Å. 1989. Semenogelin, the predominant protein in human semen. *J Biol Chem 264*:1894–1900.
Lilja H, Christensson A, Dahlén U, Matikainen MT, Nilsson O, Pettersson K, Lövgren T. 1991. Prostate-specific antigen in human serum occurs predominantly in complex with α_1-antichymotrypsin. *Clin Chem 37*:1618–1625.
Loebermann H, Tokuoha R, Deisenhofer J, Huber R. 1984. α_1-proteinase inhibitor. *J Mol Biol 177*:531–536.
Lövgren J, Piironen T, Övermo C, Dowell B, Karp M, Pettersson K, Lilja H, Lundwall Å. 1995. Production of recombinant PSA and hK2 and analysis of their immunologic cross-reactivity. *Biochem Biophys Res Commun 213*:888–895.
Lundwall Å, Lilja H. 1987. Molecular cloning of human prostate specific antigen cDNA. *FEBS Lett 214*:317–322.
Madison EL, Goldsmith EJ, Gerard RD, Gething MJH, Sambrook JF. 1989. Serpin-resistant mutants of human tissue-type plasminogen activator. *Nature 339*:721–724.
Madison EL, Goldsmith EJ, Gething MJH, Sambrook JF, Gerard RD. 1990. Restoration of serine protease-inhibitor interaction by protein engineering. *J Biol Chem 265*:21423–21426.
Meyer E, Cole G, Radhakrishnan R, Epp O. 1988. Structure of native porcine pancreatic elastase at 1.65 Å resolution. *Acta Crystallogr B 44*:26–38.
Monne M, Croce CM, Yu H, Diamandis EP. 1994. Molecular characterization of prostate-specific antigen messenger RNA expressed in breast tumors. *Cancer Res 54*:6344–6347.
Oesterling JE. 1991. Prostate-specific antigen: A critical assessment of the most useful tumor marker for adenocarcinoma of the prostate. *J Urol 145*:907–923.
Perona JJ, Craik CS. 1995. Structural basis of substrate specificity in the serine proteases. *Protein Sci 4*:337–360.
Pettersson K, Piironen T, Seppälä M, Liukkonen L, Christensson A, Matikainen MT, Suonpää M, Lövgren T, Lilja H. 1995. Free and complexed prostate-specific antigen (PSA): In vitro stability, epitope map, and development of immunofluorometric assays for specific and sensitive detection of free PSA and PSA–α_1-antichymotrypsin complex. *Clin Chem 41*:1–9.
Ponder JW, Richards FM. 1987. Tertiary templates for proteins: Use of packing criteria in the enumeration of allowed sequences for different structural classes. *J Mol Biol 193*:775–791.
Radtke KP, Fernández JA, Villoutreix BO, Greengard JS, Griffin JH. 1995. Characterization of a cDNA for Rhesus monkey protein C inhibitor. Ev-

idence for N-terminal involvement in heparin stimulation. *Thromb Haemost 74*:1079–1087.
Riegman PHJ, Vliestra RJ, Suurmeijer J, Cleutjens CBJM, Trapman J. 1992. Characterization of the human kallikrein locus. *Genomics 14*:6–11.
Schaller J, Akiyama K, Tsuda R, Hara M, Marti T, Rickli E. 1987. Isolation, characterization and amino-acid sequence of gamma-seminoprotein, a glycoprotein from human seminal plasma. *Eur J Biochem 170*:111–120.
Schechter I, Berger A. 1967. On the size of the active site in proteases. I. Papain. *Biochem Biophys Res Commun 27*:157–162.
Schedlich LJ, Bennetts B, Morris BJ. 1987. Primary structure of a human glandular kallikrein gene. *DNA 6*:429–437.
Schreuder HA, de Boer B, Dijkema R, Mulders J, Theunissen HJM, Grootenhuis PDJ, Hol WG. 1994. The intact and cleaved human antithrombin III complex as a model for serpin-proteinase interactions. *Nature Struct Biol 1*:48–54.
Sharp K, Honig B. 1990. Electrostatic interactions in macromolecules: Theory and applications. *Annu Rev Biophys Chem 19*:301–332.
Sheehan JP, Sadler JE. 1994. Molecular mapping of the heparin-binding exosite of thrombin. *Proc Natl Acad Sci USA 91*:5518–5522.
Shenkin PS, Yarmush DL, Fine RM, Wang H, Levinthal C. 1987. Predicting antibody hypervariable loop conformation I. Ensembles of random conformations for ringlike structures. *Biopolymers 26*:2053–2085.
Shirk RA, Elisen MGLM, Meijers JCM, Church FC. 1994. Role of the H helix in heparin binding to protein C inhibitor. *J Biol Chem 269*:28690–28695.
Spassov VZ, Karshikov AD, Atanasov BP. 1989. Electrostatic interactions in proteins. A theoretical analysis of lysozyme ionization. *Biochim Biophys Acta 999*:1–6.
Stein PE, Leslie AG, Finch JT, Turnell WG, Mc Laughlin PJ, Carrell RW. 1990. Crystal structure of ovalbumin as a model for the reactive centre of serpins. *Nature 347*:99–102.
Stein PE, Leslie AGW, Finch JT, Carrell RW. 1991. Crystal structure of uncleaved ovalbumin at 1.95 Å resolution. *J Mol Biol 221*:941–959.
Stenman UH, Leinonen J, Alfthan H, Ranniko S, Tuhkanen K, Alfthan O. 1991. A complex between prostate-specific antigen and α_1-antichymotrypsin is the major form of prostate-specific antigen in serum of patients with prostatic cancer. *Cancer Res 51*:222–226.
Struthers RS, Kitson DH, Hagler AT. 1991. Predicted three-dimensional structure of the protease inhibitor domain of the Alzheimer's disease β-amyloid precursor. *Proteins Struct Funct Genet 9*:1–11.
Sunnerhagen M, Forsen S, Hoffren AM, Drakenberg T, Teleman O, Stenflo J. 1995. Structure of Ca^{2+}-free GLA domain sheds light on membrane binding of blood coagulation proteins. *Nature Struct Biol 2*:504–509.
Suzuki K, Nishioka J, Hashimoto S. 1983. Protein C inhibitor: Purification from human plasma and characterization. *J Biol Chem 258*:163–168.
Vihinen M. 1994. Modeling of prostate specific antigen and human glandular kallikrein structures. *Biochem Biophys Res Commun 204*:1251–1256.
Villoutreix BO, Getzoff ED, Griffin JH. 1994a. A structural model for the prostate disease marker prostate-specific antigen. *Protein Sci 3*:2033–2044.
Villoutreix BO, Spassov VZ, Atanasov BP, Herve G, Ladjimi MM. 1994b. Structural modeling and electrostatic properties of aspartate transcarbamylase from *Saccharomyces cerevisiae*. *Proteins Struct Funct Genet 19*:230–243.
Warshel A, Åqvist J. 1991. Electrostatic energy and macromolecular function. *Annu Rev Biophys Biophys Chem 20*:267–298.
Watt KWK, Lee PJ, Timkulu TM, Chan WP, Loor R. 1986. Human prostate-specific antigen: Structural and functional similarity with serine protease. *Proc Natl Acad Sci USA 83*:3166–3170.
Wei A, Rubin H, Cooperman BS, Christianson DW. 1994. Crystal structure of an uncleaved serpin reveals the conformation of an inhibitory reactive loop. *Nature Struct Biol 1*:251–258.
Wright HT, Qian HX, Huber R. 1990. Crystal structure of plakalbumin, a proteolytically nicked form of ovalbumin. *J Mol Biol 213*:513–528.
Young CYF, Andrews PE, Montgomery BT, Tindall DJ. 1992. Tissue-specific and hormonal regulation of human prostate-specific glandular kallikrein. *Biochemistry 31*:818–824.
Yu H, Diamandis EP. 1995. Prostate specific antigen in milk of lactating women. *Clin Chem 41*:54–58.